Inorganic Chemistry

Article

pubs.acs.org/IC

Reversible Hydride Transfer to *N,N′*-Diarylimidazolinium Cations from Hydrogen Catalyzed by Transition Metal Complexes Mimicking the Reaction of [Fe]-Hydrogenase

Masahiro Hatazawa,[†] Naoko Yoshie,[†] and Hidetake Seino*[,‡]

[†]Institute of Industrial Science, The University of Tokyo, Komaba, Meguro-ku, Tokyo 153-8505, Japan

[‡]Faculty of Education and Human Studies, Akita University, Tegata-Gakuenmachi, Akita 010-8502, Japan

Supporting Information

ABSTRACT: [Fe]-hydrogenase is a key enzyme involved in methanogenesis and facilitates reversible hydride transfer from H_2 to N^5,N^{10}-methenyltetrahydromethanopterin (CH-H_4MPT$^+$). In this study, a reaction system was developed to model the enzymatic function of [Fe]-hydrogenase by using *N,N′*-diphenylimidazolinium cation (**1**$^+$) as a structurally related alternative to CH-H_4MPT$^+$. In connection with the enzymatic mechanism via heterolytic cleavage of H_2 at the single metal active site, several transition metal complex catalysts capable of such activation were utilized in the model system. Reduction of **1**[BF_4] to *N,N′*-diphenylimidazolidine (**2**) was achieved under 1 atm H_2 at ambient temperature in the presence of an equimolar amount of NEt_3 as a proton acceptor. The proposed catalytic pathways involved the generation of active hydride complexes and subsequent intermolecular hydride transfer to **1**$^+$. The reverse reaction was accomplished by treatment of **2** with $HNMe_2Ph^+$ as the proton source, where [(η^5-C_5Me_5)Ir{(*p*-$MeC_6H_4SO_2$)NCHPhCHPhNH}] was found to catalyze the formation of **1**$^+$ and H_2 with high efficiency. These results are consistent with the fact that use of 2,6-lutidine in the forward reaction or 2,6-lutidinium in the reverse reaction resulted in incomplete conversion. By combining these reactions using the above Ir amido catalyst, the reversible hydride transfer interconverting **1**$^+$/H_2 and **2**/H^+ was performed successfully. This system demonstrated the hydride-accepting and hydride-donating modes of biologically relevant N-heterocycles coupled with proton concentration. The influence of substituents on the forward and reverse reactivities was examined for the derivatives of **1**$^+$ and **2** bearing one *para*-substituted *N*-phenyl group.

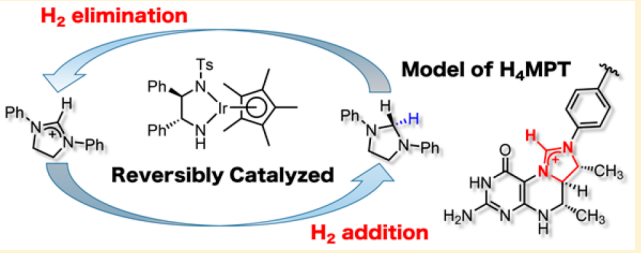

INTRODUCTION

Methanogenesis is an energy-yielding metabolic process in methanogenic archaea, accompanied by the production of methane.[1] One of the major methanogenic pathways exploits the reaction of CO_2 with H_2, which comprises of a series of enzymatic reaction steps involving some organic cofactors. As shown in Scheme 1, tetrahydromethanopterin (H_4MPT) is one of the essential cofactors employed in this system and functions as a one-carbon carrier, on which the formyl carbon is bound and reduced in two steps to the methyl level. Metabolism of H_2 is mediated by different subtypes of [NiFe]-hydrogenase in methanogenesis, but some of their roles can be substituted by [Fe]-hydrogenase under Ni-limiting growth conditions in some methanogens.[2] [Fe]-hydrogenase catalyzes the reversible hydride transfer from H_2 to methenyl-H_4MPT$^+$ to produce methylene-H_4MPT and a proton.[3] Crystallographic and spectroscopic analyses of [Fe]-hydrogenase revealed a unique monoiron center ligated by two CO, a guanylylpyridinol moiety, and cysteinyl residue (FeGP cofactor, Figure 1).[4] These functional and structural features are in contrast to [NiFe]- and [FeFe]-hydrogenases, which split H_2 into protons and electrons at the dinuclear catalytic sites and transfer electrons through the iron−sulfur cluster chains.[5]

The iron center of the FeGP cofactor is proposed to be divalent and has a pseudo-octahedral geometry with an open site trans to the acyl ligand (occupied by H_2O in the crystal structure).[4] This site is thought to coordinate H_2 for heterolytic splitting, and the resulting hydride is transferred to methenyl-H_4MPT$^+$, which is located in the proximity but not directly binding to the iron. As for the proton, computational[6−8] and experimental[3c] studies support the mechanism, in which the hydroxy group of the 2-pyridinol ligand is deprotonated prior to H_2 cleavage to serve as the internal proton acceptor. As an experimental approach to provide an insight into the enzymatic mechanism, a number of iron complexes have been synthesized as structural models for the FeGP cofactor since the elucidation of its detailed structure.[9,10] However, studies on reactivity of such model complexes toward the substrates relevant to [Fe]-hydrogenase have arisen lately. The groups of Shima and Hu demonstrated that some of the synthetic mimics can be used to

Received: March 28, 2017

DOI: 10.1021/acs.inorgchem.7b00806
Inorg. Chem. XXXX, XXX, XXX−XXX

Scheme 1. Selected Reaction Steps in the Methanogenic Pathway Utilizing CO_2 and H_2

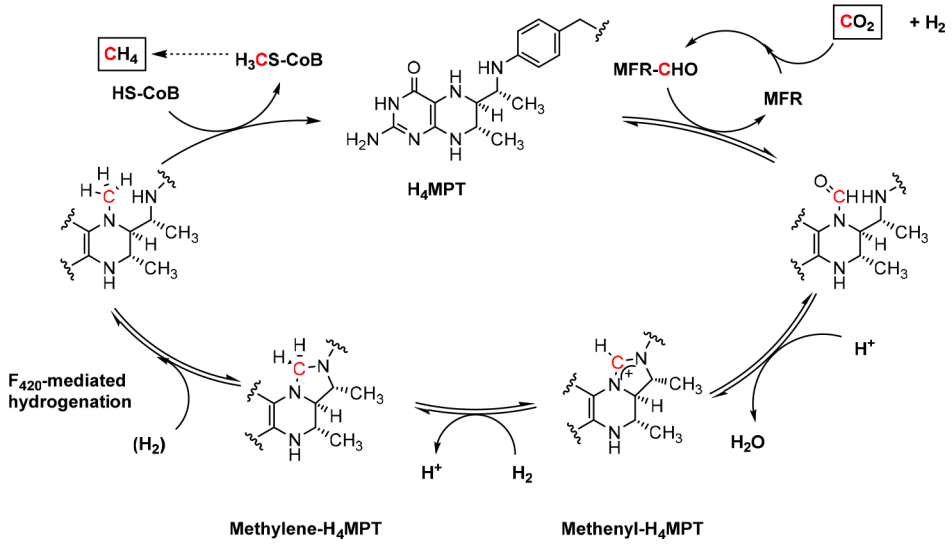

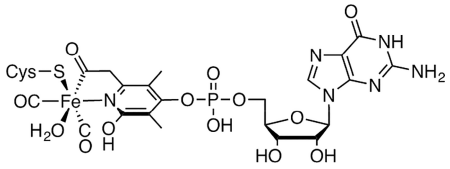

Figure 1. FeGP cofactor of [Fe]-hydrogenase.

reconstitute active [Fe]-hydrogenase from its apoenzyme.[3c] In the case of the model complex alone, even the heterolytic activation of H_2 molecules was recently achieved, using the iron complex bearing a pyridine−acyl unit and a PNP ligand.[10h] The amine moiety in the PNP ligand served as a proton acceptor, and some catalytic turnover in hydrogenation of an aldehyde was demonstrated. Rose and co-workers developed the iron complex having the *fac*-*C*(acyl),*N*,*S* coordination motif supported by an anthracene scaffold, which could heterolyze H_2 (or D_2) to form an iron−hydride (or deuteride) species.[10i] By use of this complex, they also conducted catalytic hydride abstraction from 1,2,3-triarylimidazolidine, a biomimetic model for methylene-H_4MPT.

Despite the above example, investigation into the model reactions using certain molecules resembling the organic substrates of [Fe]-hydrogenase are still limited, even if nonbiomimetic catalysts are included.[11−13] Such attempts are sometimes informative to elucidate the functions of enzymes.[9c,14] Corr et al. reported that a bicyclic amidinium dication is hydrogenated with H_2 (52 psi) and Pd on carbon, resulting in the ring-opening via C−N bond cleavage.[12] Kalz et al. examined heterolytic splitting of H_2 using a combination of Lewis basic Ru complexes and 1,2,3-triarylimidazolinium salts as proton- and hydride-acceptors, respectively.[13] The imidazolinium cations in the latter study were structurally related to methenyl-H_4MPT$^+$, except for the substituent at the C-2 position to avoid some side reactions, and the same molecular design was applied in the Rose's system performing the reverse reaction.[10i] Because the reaction center of methenyl-H_4MPT$^+$ is the C-2 atom of the imidazolinium ring, C-2 unsubstituted models should exhibit comparatively similar reactivity. In this study, we selected *N*,*N*′-diphenylimidazolinium (**1**$^+$) as the representative model substrate and investigated hydride transfer to **1**$^+$ from molecular H_2 by using homogeneous transition metal catalysts (Figure 2). The reverse conversion was also carried out via the combination of the proton source with *N*,*N*′-

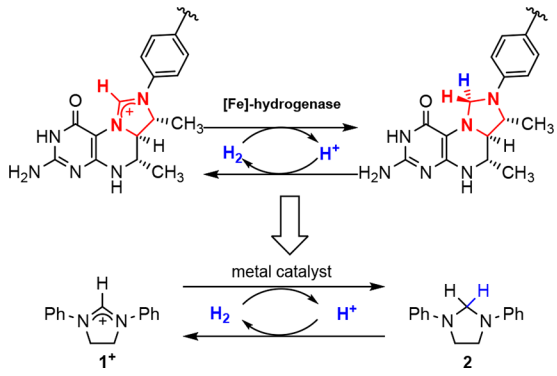

Figure 2. Reversible reaction catalyzed by [Fe]-hydrogenase and model reactions designed in this study.

diphenylimidazolidine (**2**), the molecule corresponding to methylene-H_4MPT. Although a related approach has been previously applied in a density functional theory study,[15] experimental confirmation has not yet been undertaken.

While a multiscale modeling of the [Fe]-hydrogenase/methenyl-H_4MPT$^+$ complex proposed the mechanism that hydride is transferred to methenyl-H_4MPT$^+$ from the iron-coordinated H_2 without forming a hydride ligand,[7b] synthetic functional models for the FeGP cofactor were hitherto hypothesized to operate via the iron−hydride intermediates.[10h,i] Formation of the metal−hydride intermediate in heterolysis of H_2 by transition metal catalysts is widely accepted.[16] Our investigations have focused on the catalyst precursors, which split coordinated H_2 heterolytically and transfer the resulting reactive hydride to substrates in an intermolecular manner (Figure 3). The arene−Ru amido complex [(η^6-*p*-cymene)Ru((*R*,*R*)-Tsdpen−H)] (**3**; Tsdpen−H = (*p*-Me$C_6H_4SO_2$)NCHPhCHPhNH) and its cyclopentadienyl−Ir analogue [Cp*Ir((*R*,*R*)-Tsdpen−H)] (**4**; Cp* = η^5-C_5Me_5) are representative bifunctional catalysts, in which the amido nitrogen atom acts as the internal basic site. These complexes are effective for the hydrogenation of polar unsaturated bonds such as C═O and C═N.[17,18] Another Ir

DOI: 10.1021/acs.inorgchem.7b00806
Inorg. Chem. XXXX, XXX, XXX−XXX

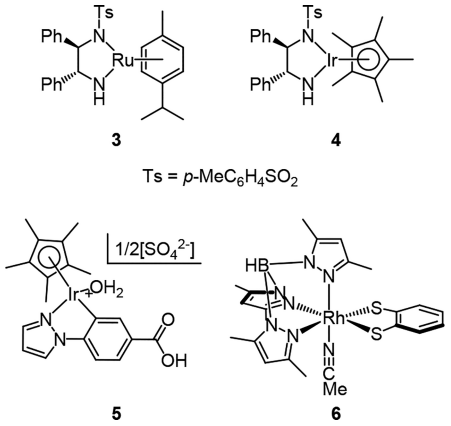

Figure 3. Representative catalyst precursors examined in this study.

complex **5** possessing a C−N chelate has been reported to catalyze the reversible reduction of NAD^+.[19] The Rh benzenedithiolato complex $[Tp^{Me2}Rh(1,2\text{-}S_2C_6H_4)(MeCN)]$ (**6**; Tp^{Me2} = hydrotris(3,5-dimethylpyrazol-1-yl)borate) exhibits salient chemoselectivity in the hydrogenation of C═N bonds.[20] Both **5** and **6** have been established to generate active hydride intermediates under ambient conditions through proton release from the coordinated H_2.

RESULT AND DISCUSSION

Catalytic Hydride Addition to *N,N′*-Diphenylimidazolinium 1^+. Hydrogenation experiments of $1[BF_4]$ were conducted under atmospheric pressure of H_2. Because hydride transfer to 1^+ was conjugated with proton release, this reaction proceeded only in the presence of an adequate proton acceptor. Triethylamine was found to be suitable for this purpose (*vide infra*), and an equimolar amount to 1^+ was used in the reactions. Activity of each catalyst complex (1 mol %) was examined in *i*PrOH and THF, and the reaction medium giving higher conversion was collected in Table 1 (see Supporting Information Table S1 for full data). Because of the poor solubility of $1[BF_4]$ in these solvents, all reaction mixtures formed suspensions in the initial stage, while product **2** dissolved well in THF but sparingly in *i*PrOH.

Catalyst **3** was moderately active in *i*PrOH solvent at 35 °C, but the conversion rate decreased considerably at 25 °C (entries 1, 2). Higher activity than **3** was observed for the Ir analogue **4** and another Ir complex **5**, which achieved satisfactory conversions at 25 °C (entries 3, 4). The fastest catalytic rate was exhibited by **6** in THF solvent (approximately 4-fold faster than **4** and **5**; entries 5, 6). Although we anticipated that the added base would deprotonate 1^+ at the 2-C position to generate the N-heterocyclic carbene species, the experimental results confirmed that all consumed 1^+ was exclusively converted into **2** without any such side reactions. NMR analyses of nonvolatile materials in the reaction mixture revealed that nearly equimolar amounts of **2** and triethylammonium salt were produced as a result of heterolytic H_2 cleavage.

It has been previously shown that 1,3-disubstituted imidazolinium cations are reduced to the corresponding imidazolidines by relatively strong reducing agents such as Zn/HCl,[21] $NaBH_4$,[22] or $LiAlH_4$.[22,23] The results in this study revealed that such conversion can be performed under very mild conditions by the catalytic reaction using H_2 as a reducing agent.[24] To gain an insight into the mechanisms of the catalysis, the effects of proton acceptors and solvents were further investigated for the representative catalysts **4** and **6**.

Effects of Bases and Solvents on Hydride Addition Catalyzed by Ir Amido Complex 4. Conversion of $1[BF_4]$ into **2** catalyzed by **4** was examined under various conditions as listed in Table 2. For the reactions under a H_2 atmosphere in *i*PrOH, essentially no reaction took place in the absence of basic additives (entry 1). It was confirmed that the amount of base limited the conversion (entry 2), indicating a demand for a

Table 1. Comparison of Catalysts for Hydride Addition to $1[BF_4]$ Utilizing H_2[a]

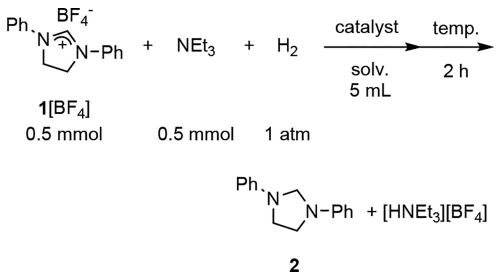

entry	catalyst	solvent	yield of **2** [%][b]	recovery of $1[BF_4]$ [%][b]
1	**3**	*i*PrOH	32	68
2[c]	**3**	*i*PrOH	86	14
3	**4**	*i*PrOH	92	8
4	**5**	*i*PrOH	97	3
5	**6**	THF	100	0
6[d]	**6**	THF	94	6

[a]Conditions: $1[BF_4]$ (0.50 mmol), NEt_3 (0.50 mmol), catalyst (5 μmol), solvent (5 mL), H_2 (1 atm), 25 °C, 2 h, or otherwise stated. [b]Determined by ^1H NMR spectroscopy. [c]Conducted at 35 °C. [d]Reacted for 30 min.

Table 2. Examination of Reaction Conditions in Hydride Addition to $1[BF_4]$ Catalyzed by 4[a]

entry	base	solvent	yield of **2** [%][b] (time/h)
H_2 atmosphere			
1	none	*i*PrOH	1 (24)
2	NEt_3[c]	*i*PrOH	50 (8)
3	NEt_3	*i*PrOH	21 (0.5), 92 (2)
4	Lut	*i*PrOH	31 (2), 84[d] (24)
5	NMe_2Ph	*i*PrOH	7[e] (24)
6	NEt_3	EtOH	65 (0.5), 100 (2)
7	NEt_3	*t*-BuOH[f]	0 (2)
8	NEt_3	THF	12 (2)
9	NEt_3	CH_2Cl_2	5 (2)
N_2 atmosphere			
10	NEt_3	*i*PrOH	14 (0.5), 40 (2), 96 (24)
11	NEt_3	EtOH	61 (0.5), 91 (2)
12	Lut	*i*PrOH	2 (24)

[a]Conditions: $1[BF_4]$ (0.50 mmol), base (0.50 mmol), **4** (5 μmol), solvent (5 mL), 1 atm, 25 °C, or otherwise stated. Lut = 2,6-dimethylpyridine. [b]Determined by ^1H NMR spectroscopy. The consumed amount of $1[BF_4]$ was equivalent to the yield of **2** for every reaction except where indicated. Data of different reaction times were obtained from independent reaction batches. [c]Conducted with 0.50 equiv of NEt_3. Recovery of 1^+ was 47%. [d]In addition to unreacted 1^+ (5%), uncharacterized byproducts were observed. [e]In addition to unreacted 1^+ (79%), uncharacterized byproducts were observed. [f]Conducted at 35 °C.

DOI: 10.1021/acs.inorgchem.7b00806
Inorg. Chem. XXXX, XXX, XXX−XXX

Scheme 2. Plausible Mechanisms for Hydride Transfer to 1^+ Mediated by Ir Catalyst 4

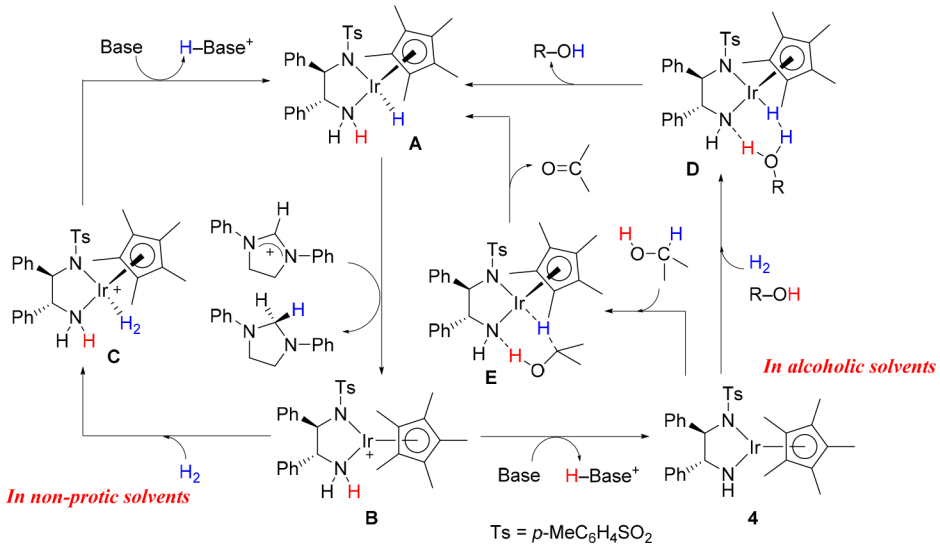

stoichiometric amount of proton acceptor. The reaction rates and proportions were revealed to depend on the proton-accepting ability of bases (entries 3−5). The reaction using 2,6-dimethylpyridine (Lut) proceeded more slowly than that with NEt_3, while the use of NMe_2Ph resulted in very poor conversion. These results are consistent with the order of pK_a units for the conjugate acids of these bases (14.9, 9.5, and 7.2, for NEt_3, Lut, and NMe_2Ph, respectively, in THF).[25] Furthermore, catalytic rates were considerably affected by solvents. The reaction under H_2 using NEt_3 was somewhat faster in EtOH than in *i*PrOH (entry 6 vs 3) but very slow in *t*-BuOH, THF, and CH_2Cl_2 (entries 7−9). These solvent effects indicate that EtOH and *i*PrOH may act as hydride donors, and in fact, **4** is well-known to catalyze transfer-hydrogenation, which utilizes primary and secondary alcohols as hydrogen sources.[18,26] To verify this hypothesis, the above reactions in EtOH and *i*PrOH were carried out under nitrogen gas. The conversion rates in EtOH exhibited no significant differences between H_2 and N_2 atmosphere, indicating that the reactions proceeded majorly via a transfer-hydrogenation mechanism in this solvent (entry 6 vs 11). As for the reactions in *i*PrOH, turnover frequency partly decreased under N_2, while final conversions were almost equal to each other (entry 3 vs 10). In contrast, the reaction utilizing Lut as the proton acceptor only minimally proceeded in the absence of H_2 (entry 12). This suggests that the combination of *i*PrOH with Lut exerts weaker hydride-donating ability than the sets of H_2−Lut or *i*PrOH−NEt_3.

The catalytic function of **4** in the hydride transfer to $\mathbf{1}^+$ may be relevant to that in the hydrogenation of imines, which has been previously established to proceed via ionic mechanisms. Previous studies utilizing **4** and analogous bifunctional catalysts showed that the imine substrate is preactivated by protonation or coordination of Lewis-acidic metal ions and that hydride is transferred to the resulting iminium carbon from the hydride complex derived from **4** and H_2 (structure **A** in Scheme 2).[27,28] Analogous to this mechanism, hydride transfer to $\mathbf{1}^+$ is thought to proceed via the routes shown in Scheme 2. The key metal species is the hydride complex **A**, from which the hydride is transferred to $\mathbf{1}^+$ without coordination to the metal center to produce **2** and a cation **B**. This step was supported by NMR analysis, as the addition of $\mathbf{1}[BF_4]$ (1.3 equiv) to a CD_2Cl_2 solution of **A** resulted in the immediate disappearance of the hydride signal and formation of **2** (equimolar amount to **A**).[29]

There are a number of possible routes regenerating **A** in the catalytic cycle. Complexation of the coordinatively unsaturated **B** with H_2 forms the intermediate **C**, and the subsequent deprotonation from the η^2-H_2 ligand by an external base produces the hydride complex **A**. Conversion of **B** to **A** has been reported to occur rapidly at 1 atm H_2 in the presence of an appropriate base such as NEt_3.[28,30,31] In contrast, the direct action of the base on **B** causes proton elimination from the amine ligand to give **4**,[30] which is convertible into **A** through heterolysis of H_2 at the Ir−amide moiety. It was previously shown that direct addition of molecular H_2 to **4** in aprotic solvents is very slow and is accelerated by a catalytic amount of acid because the pathway via species **B** and **C** becomes accessible. In THF or CH_2Cl_2 solution, most metal species are considered to be in the resting state of **4** via deprotonation of **B** in the presence of excess base (NEt_3/cat ∼ 100 in the initial stage), as is indicated from the reddish purple color characteristic of **4**. Slow regeneration of the active species **A** from **4** in these solvents may explain the low catalytic turnovers, and thus the use of preformed **A** instead of **4** as the catalyst precursor did not result in any improvement.

In contrast, some alcoholic solvents have been found to effectively assist the addition of H_2 to **4**, which has been proposed to occur via proton relay mechanisms involving the amido ligand, H_2, and an alcohol molecule (transition state **D**).[32] In addition, **4** can eliminate H_2 from an alcohol molecule to form **A** via the concerted transition state **E** as established for the mechanisms of transfer hydrogenation.[16,26] Competition between H_2-hydrogenation and transfer-hydrogenation in alcoholic solvents has been observed for certain asymmetric ketone reduction systems catalyzed by **4** and the analogue [Cp*Ir((*S*,*S*)-Msdpen−H)] (**4′**; Msdpen−H = $(MeSO_2)$NCHPhCHPhNH).[32d] When the reduction of $\mathbf{1}^+$ is conducted at 1 atm H_2 in *i*PrOH solvent, both pathways utilizing H_2 or alcohol as the hydrogen source presumably operate in parallel to generate **A**. The extent of each hydrogenation route is roughly estimated by comparing the catalytic turnovers in the presence and the absence of hydrogen gas, and the rates of two routes do not appear to be very different from each other under 1 atm H_2 (Table 2, entry 3 vs 10); however, the rate of H_2-hydrogenation

DOI: 10.1021/acs.inorgchem.7b00806
Inorg. Chem. XXXX, XXX, XXX−XXX

is expected to increase depending on H_2 pressure. When the proton acceptor is Lut, the reaction takes place solely with the uptake of H_2 molecules, likely because of thermodynamic disadvantages in dehydrogenation of alcohol to produce ketone concomitantly with the relatively strong acid $HLut^+$. In this case, the apparent contribution of *i*PrOH is to assist heterolytic cleavage of H_2 by forming a hydrogen bonding network **D**.

Experiments using deuterated 2-propanols also provided evidence for the above H_2-hydrogenation and transfer-hydrogenation pathways under H_2. When reaction was conducted in $(CD_3)_2CDOD$ under 1 atm H_2, deuterium was incorporated only at the C-2 position of the produced **2**. The isotopic distribution of the 2-methylene group was CH_2:CHD:CD_2 = 42:47:11, and the existence of the CH_2 isotopomer proved H transfer from H_2 (see Supporting Information Figures S1 and S3 for the spectra). The same reaction in $(CH_3)_2CDOH$ also gave the deuterated product with the ratio CH_2:CHD:CD_2 = 83:17:0, supporting α-D abstraction from the solvent (Supporting Information Figure S2). Although the ratios of H-transfer from H_2 to α-D-transfer from 2-propanol are seemingly incompatible between these solvents, it is mostly because of the exchange with the hydroxy H/D atom via the reverse reaction of the Ir hydride/deuteride (**A**) with alcohol molecule to form **4** via **D**.

Solvent Effects on Hydride Addition Catalyzed by Rh Dithiolato Complex 6. The influence of bases and solvents on hydride transfer to **1**[BF_4] utilizing precatalyst **6** is summarized in Table 3. The effects of basic additives were

Table 3. Effects of Bases and Solvents on Hydride Addition to 1[BF_4] Catalyzed by 6[a]

entry	base	solvent	conversion [%][b]
1	NEt_3	THF	100
2	Lut	THF	21[c]
3[d]	NMe_2Ph	THF	1
4	NEt_3	EtOH	66
5[e]	NEt_3	EtOH	4
6	NEt_3	CH_2Cl_2	98
7	NEt_3	toluene	24

[a]Conditions: **1**[BF_4] (0.50 mmol), base (0.50 mmol), **6** (5 μmol), solvent (5 mL), 1 atm H_2, 25 °C, 2 h, or otherwise stated. [b]NMR yield of **2** (confirmed to be equivalent to the consumed amount of **1**[BF_4] for every reaction). [c]Yield after 24 h was 23%. [d]Reacted for 24 h. [e]Conducted under N_2 atmosphere at 50 °C.

compared for the reactions in THF (entries 1−3). While the reaction using NEt_3 rapidly reached complete conversion, use of Lut resulted in termination at low yield (~23%) likely owing to the equilibration between reactants and products. Because the reaction utilizing Lut and catalyst **4** showed relatively high yield (84%) in *i*PrOH medium (*vide supra*), the solvents may significantly affect equilibrium. In contrast to **4**, **6** showed higher catalytic activity in THF than in EtOH (entries 1 and 4) and consumed only a small amount of EtOH as a hydrogen source (entry 5). A good conversion rate was also achieved in CH_2Cl_2 solvent (entry 6), while the activity was very low in the nonpolar toluene medium (entry 7).

In our previous study, we proposed that **6** catalyzes the hydrogenation of imines via ionic mechanisms, in which protonated imine undergoes hydride transfer from the metal hydride species.[20] This catalytic pathway is supported by the observation that **6** smoothly reacts with H_2 and NEt_3 to produce the anionic hydride $[Tp^*RhH(1,2\text{-}S_2C_6H_4)]^-$ (**F**) and $HNEt_3^+$. As illustrated in Scheme 3, the conversion of $\mathbf{1}^+$ to **2** is

Scheme 3. Plausible Mechanisms for Hydride Transfer to $\mathbf{1}^+$ Mediated by Rh Catalyst 6

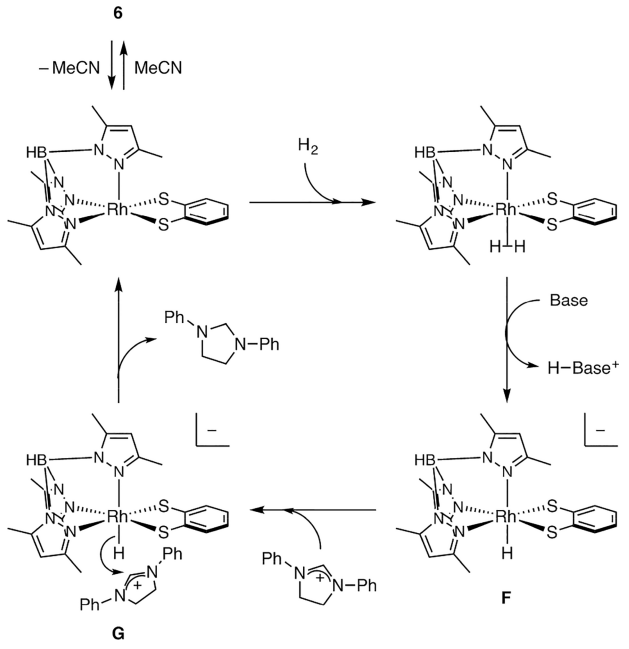

thought to proceed via the same fundamental route. Hydride transfer from **F** to the methenyl carbon of $\mathbf{1}^+$ presumably occurs without coordination (transition state **G**). Generation of the ionic hydride **F** may be retarded in nonpolar or protic media to decrease catalytic turnover. The catalytic cycle proposed here is essentially analogous to the left cycle in Scheme 2 and may be applicable to the reaction catalyzed by **5**.[19]

Catalytic Hydrogen Evolution from *N,N′*-Diphenylimidazolidine 2 and Proton. After evaluating hydride transfer from H_2 to $\mathbf{1}^+$, efforts to model the reversible catalysis of [Fe]-hydrogenase focused on the reverse reaction to form H_2, utilizing **2** as the hydride donor. The equilibrium of the reaction system can be shifted toward the reverse direction by adjusting the proton concentration, and the required acidity was reasonably estimated from the effects of the bases in the forward reaction. Because the above hydride transfer process proceeded to completion when NEt_3 was used and reached equilibrium when Lut was used, the proton donors should not be weaker than $HLut^+$ (pK_a = 9.5 (THF))[25] to drive hydride elimination from **2**. This hypothesis was tested by the reactions using **4** as the catalyst precursor (Table 4, entries 1−3). When a mixture of **2** and an equimolar amount of [HLut][BF_4] (**7**) in *i*PrOH was placed in a closed reaction vessel with 1 mol % **4** under vacuum (entry 1), 51% yield of $\mathbf{1}^+$ was obtained after 20 h at 35 °C concomitantly with the evolution of H_2 (0.28 equiv to **2** charged). This deficient conversion rate was attributable to the equilibration of the reaction system (0.10−0.12 atm H_2 in gas phase), as the yields were not greatly affected by catalyst loading (entry 2). In place of **7**, the use of a stronger acid [$HNMe_2Ph$][BF_4] (**8**) effectively improved the conversion rate, resulting in high yield of $\mathbf{1}^+$ at 25 °C after 2 h (entry 3). The reaction also produced H_2 in a yield comparable to $\mathbf{1}^+$, which originated from the hydride in **2** and proton in **8** (up to 0.40 atm partial pressure of H_2 in gas phase). It was confirmed that

DOI: 10.1021/acs.inorgchem.7b00806
Inorg. Chem. XXXX, XXX, XXX−XXX

Table 4. Reactions of 2 with Proton in the Presence of Several Hydrogenation Catalysts[a]

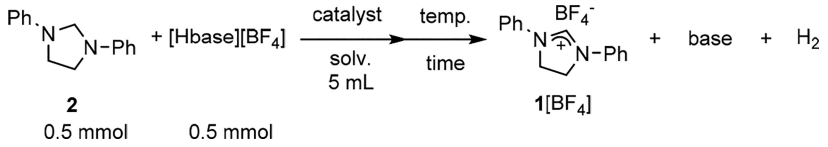

entry	catalyst	H^+ source	solvent	temp [°C]	time [h]	yield [%] $1[BF_4]$[b]	yield [%] H_2[c]	recovery of 2 [%][b]
1	**4**	**7**	*i*PrOH	35	20	51	28	36
2	**4**[d]	**7**	*i*PrOH	35	20	54	26	25
3	**4**	**8**	*i*PrOH	25	2	89	85	0
4	**4**	**8**	EtOH	25	2	33	18	57
5	**4**	**8**	THF	25	2	33	17	45
6	**3**	**8**	*i*PrOH	25	2	45	19	48
7	**3**	**8**	*i*PrOH	35	2	100	95	0
8	**5**	**8**	*i*PrOH	35	1	58	21	0
9	**5**	HBF_4[e]	*i*PrOH	35	1	68	60	0
10	**6**	**8**	THF	35	20	8	3	49
11	**6**	**8**	*i*PrOH	35	20	48	5	0

[a]Standard conditions: **2** (0.50 mmol), H^+ source (0.50 mmol), catalyst (5 μmol), solvent (5 mL), under vacuum, or otherwise stated. [b]Determined by ^1H NMR spectroscopy. [c]H_2 in the gas phase determined by GC analyses. [d]Conducted with 2.5 mol % catalyst loading. [e]Aqueous HBF_4 (0.50 mmol) was used.

Scheme 4. Plausible Catalytic Cycle for Generation of H_2

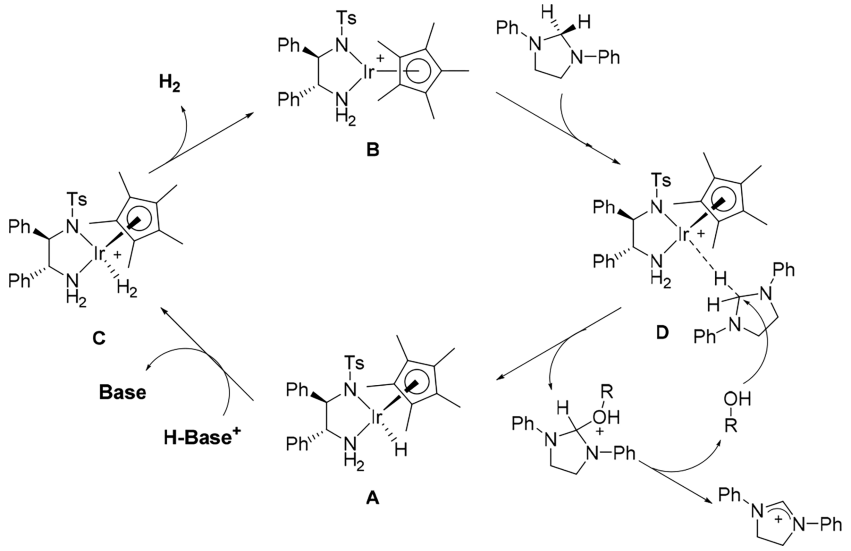

H_2 elimination from *i*PrOH was negligible under these reaction conditions (0.6 equivalent to **4** after 24 h at 35 °C) from the blank test in which **8** was reacted with 1 mol % **4** in *i*PrOH without adding imidazolidine **2**.

Because $HNMe_2Ph^+$ (pK_a = 7.2 (THF))[25] was found to be sufficiently acidic to completely convert **2** to $\mathbf{1}^+$ and H_2, equimolar reactions containing **2** and **8** were examined under various conditions. The catalytic turnover of catalyst **4** was greater in *i*PrOH solvent than in EtOH or THF (entries 3–5). Although the activity of the analogous Ru catalyst **3** was slightly lower than that of **4**, sufficient conversion was observed at a relatively high temperature (entries 6, 7). The reaction utilizing catalyst **5** was accompanied by uncharacterized side reactions and resulted in poor yields of both $\mathbf{1}^+$ and H_2 despite relatively rapid consumption of **2** (entry 8). Using aqueous HBF_4 as the proton source had only a small influence on the yield of $\mathbf{1}^+$, while the evolution of H_2 appreciably increased (entry 9). The Rh catalyst **6** was less reactive and formed very little H_2 even after consumption of a fair portion of **2** (entries 10, 11). Uncharacterized side products were observed by NMR measurement in both cases, which require further investigation. In conclusion, among the examined catalysts, the most efficient for H_2 evolution via hydride elimination from **2** was confirmed to be **4**, which exhibited high activity even at ambient temperature.

As illustrated in Scheme 4, the reaction pathway catalyzed by **4** was thought to follow the reverse direction of the left cycle of Scheme 2. NMR measurement in CD_2Cl_2 revealed that the Ir species existed in the protonated form **B** in the presence of **8** (1–2 equiv). While **2** showed no interaction with **4** in CD_2Cl_2 at 25 °C, addition of **8** to this mixture resulted in gradual increases in the NMR signals of $\mathbf{1}^+$. During this change, the metal species was observed as **B**, and any hydride species such as **A** were not detectable. Lewis-acidic **B** may eliminate hydride

DOI: 10.1021/acs.inorgchem.7b00806
Inorg. Chem. XXXX, XXX, XXX–XXX

from **2**, and the resulting hydride complex **A** is immediately protonated to give **B** and H_2 via the intermediate **C**. Peris and co-workers reported that the reaction of *N*,*N*′-dibenzylimidazolidine with $[Cp^*IrCl_2(L)]$ (L = neutral $2e^-$ donor) in the presence of $Ag(CF_3SO_3)$ at 45 °C produces *N*,*N*′-dibenzylimidazolinium and the monohydride complexes $[Cp^*IrHCl(L)]$.[33] The dinuclear complex $[(Cp^*IrCl)_2(\mu\text{-}Cl)_2]$ also abstracts hydride from various *N*,*N*′-dialkylimidazolidine derivatives at room temperature to give $[(Cp^*IrCl)_2(\mu\text{-}H)_2]$. The isoelectronic half-sandwich complexes of Rh and Ru react in a similar manner. For the catalytic system in this study, the accelerated reaction rates in *i*PrOH medium may be explained by its assistance in the proton transfer step or involvement in the hydride elimination step to form an aggregating intermediate, as shown in Scheme 4 (bottom-right corner). Concerted nucleophilic attack of the alcohol molecule to the 2-C possibly decreased the activation energy of hydride transfer to the Ir center, as related adducts between imidazolinium and alkoxide are known.[34]

Catalytic hydrogen evolution as described above confirms that **2** serves as an efficient hydride donor when activated by appropriate catalysts. Including biologically essential NADH and NADPH, a large number of N-heterocyclic compounds have been identified as organo-hydride donors.[35] Despite their ability to transfer hydride to various acceptor molecules, hydride transfer to proton leading to H_2 formation is rarely observed.[36] Thorn et al. demonstrated H_2 evolution utilizing *N*,*N*′-dimethylbenzimidazoline and acetic acid as the hydride and proton donors, respectively, at room temperature in the presence of a metallic Pd catalyst.[37,38] The reaction produces the benzimidazolium cation, and derivatives with one aryl group at the 2-position react in a similar manner. In the same reaction system, Peris et al. demonstrated that *N*,*N*′-dialkylimidazolidine (alkyl = methyl, benzyl) and some related N-heterocycles can act as hydride sources.[33] These N-heterocycles have relatively high hydride-donating ability, making H_2 evolution strongly exergonic, while also making the reverse reaction difficult.[39] Less hydridic NADH can function as a reversible organic hydride in the H_2 release/storage cycle, as Fukuzumi and co-workers successfully performed H_2 evolution from NADH to give NAD^+ and the reverse reaction by switching the pH of the aqueous media.[19] These reactions were conducted under ambient conditions with **5** as the catalyst precursor. Their and our experimental results confirmed that the homogeneous transition metal catalysts that operate through an ionic hydrogenation mechanism were effective for this type of hydride transfer.[40] It is indicated that **2** has a hydride-donating ability comparable to NADH and can be replenished with hydride under moderately basic conditions (NEt_3) and atmospheric H_2 pressure.

Sequential Addition and Elimination of H_2. Organic molecules, which can reversibly release and add H_2, have gained attention as potential materials for chemical storage of hydrogen gas.[41] Numerous studies have been carried out to examine molecules containing releasable hydrogen such as cycloalkanes, saturated heterocycles, alcohols, formic acid, etc., by using various catalysts. Compared with heterogeneous catalysts, the use of homogeneous catalysts is still limited, but these reactions proceed under relatively mild conditions.[32e,42] To determine the feasibility of using $\mathbf{1}^+$ as a molecular hydride storage, sequential addition and elimination of H_2 was carried out for the reaction system combined with a proton donor/acceptor (Scheme 5). Complex **4** was selected as the single

Scheme 5. Sequential Addition and Elimination of H_2

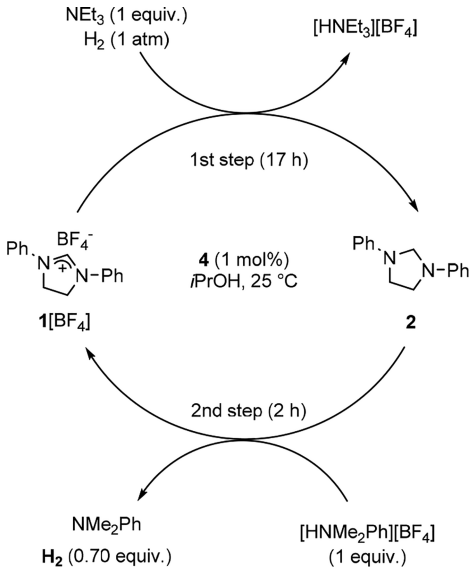

catalyst precursor in this system because it can catalyze both the forward and the reverse reactions with reasonable activities. For the H_2-addition step, a mixture of $\mathbf{1}[BF_4]$, NEt_3 (1.0 equiv), and **4** (0.01 equiv) in *i*PrOH was treated with 1 atm H_2 at 25 °C for 17 h. After freezing the resulting mixture at −196 °C and evacuation of the gas phase, the H_2-elimination step was performed by adding proton source **8**, followed by stirring under vacuum at 25 °C, to result in the release of 70% H_2 per charged $\mathbf{1}[BF_4]$ after 2 h. Although the conversion rate of $\mathbf{1}^+$ in the above H_2-addition step was high (92% after 2 h, *vide supra*), a part of hydride originated from *i*PrOH via H_2 transfer. Therefore, the reaction time must be extended to hydrogenate the resulting Me_2CO. Conducting the H_2-addition step for only 2 h resulted in a decrease of released H_2 (56% per $\mathbf{1}[BF_4]$).

Effects of Substituted Phenyl Group in Imidazolinium Cations and Imidazolidines. While H_4MPT is a specific coenzyme in methanogenesis, another biological C1 carrier, tetrahydrofolate (H_4folate), is ubiquitous in a wide range of organisms (Figure 4).[43] The structures of H_4MPT (see Scheme

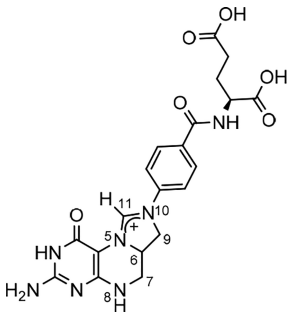

Figure 4. Structure of N^5,N^{10}-CH^+-H_4folate.

1) and H_4folate are very similar; one of the differences in their active sites is that two extra methyl groups are attached to the carbon skeleton in H_4MPT (C7 and C9 sites[44]). Another significant difference is the *para*-substituent on the benzene ring bound to the N10 atom, which is an electron-donating alkyl chain in H_4MPT and an electron-withdrawing amide carbonyl in H_4folate, giving H_4MPT derivatives more negative redox potentials than the corresponding H_4folate derivatives

DOI: 10.1021/acs.inorgchem.7b00806
Inorg. Chem. XXXX, XXX, XXX−XXX

(e.g., −70 mV difference for CH^+/CH_2 couples). In connection with the structural and functional divergences between these natural coenzymes, reactivity was investigated for the series of $\mathbf{1}^+$ and **2** analogues, one of whose phenyl groups had various substituents (X) at the *para*-position (represented as $\mathbf{1_X}^+$ and $\mathbf{2_X}$).

Hydride addition to a series of imidazolinium salts $\mathbf{1_X}[BF_4]$ was examined under 1 atm H_2 in the presence of 1 equiv of NEt_3 by using two catalytic systems (Table 5). The reactions

Table 5. Catalytic Hydride Addition to Asymmetrically Substituted Diphenylimidazolinium Salts Utilizing H_2[a]

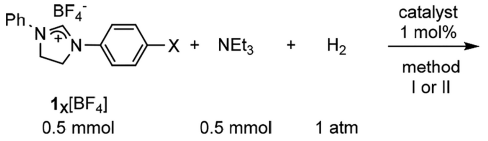

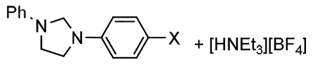

$\mathbf{2_X}$

entry	substrate	X	yield of $\mathbf{2_X}$ [%][b] method I[c]	method II[d]
1	$\mathbf{1_F}[BF_4]$	F	100	60
2	$\mathbf{1_{Cl}}[BF_4]$	Cl	98	57
3	$\mathbf{1_{Br}}[BF_4]$	Br	100	34
4	$\mathbf{1_{CF3}}[BF_4]$	CF_3	100	68
5	$\mathbf{1_{COOMe}}[BF_4]$	COOMe	79	54
6	$\mathbf{1_{CN}}[BF_4]$	CN	87[e]	22
7	$\mathbf{1}[BF_4]$	H	94	92
8	$\mathbf{1_{Me}}[BF_4]$	Me	97	45
9	$\mathbf{1_{OMe}}[BF_4]$	OMe	62[e,f]	40

[a]Common reaction conditions: $\mathbf{1_X}[BF_4]$ (0.50 mmol), NEt_3 (0.50 mmol), catalyst (5 μmol), solvent (5 mL), H_2 (1 atm), 25 °C, or otherwise stated. [b]Determined by ^1H NMR spectroscopy. [c]Catalyst **6**, THF solvent, 0.5 h, or otherwise stated. Yield reached 100% after 2 h for every entry except 6 and 9. [d]Catalyst **4**, *i*PrOH solvent, 2 h. [e]Conducted for 2 h. [f]67% yield after 24 h.

with catalyst **6** in THF (method I) were effective for converting a wide range of substituted derivatives. Halo- and trifluoromethyl-substituted imidazoliniums were converted more rapidly than the original $\mathbf{1}[BF_4]$ (entries 1−4 vs 7). Although electron-withdrawing COOMe and CN groups were expected to accelerate the incorporation of hydride, the conversion rates of these derivatives were rather slow (entries 5, 6). The presence of excess nitrile has been known to retard the catalysis of **6** due to coordination to the site of hydrogen activation.[20b] Using method I with S/C = 100, conversion into the corresponding imidazolidine $\mathbf{2_X}$ was completed within 2 h for all examined substrates except for the cyano and methoxy derivatives: reaction of the latter converged at $\mathbf{1_{OMe}}^+/\mathbf{2_{OMe}}$ = 33/67.

In contrast, transformation of any substituted $\mathbf{1_X}[BF_4]$ using **4** as the catalyst precursor in *i*PrOH (method II) resulted in lower conversion than that of nonsubstituted $\mathbf{1}[BF_4]$. The remaining substrate was unchanged, and no appreciable side reactions such as hydrogenation at the functional groups were observed under the applied conditions (1 atm H_2, 25 °C). Because a series of $\mathbf{1_X}[BF_4]$ and $\mathbf{2_X}$ are both severely insoluble in *i*PrOH at 25 °C, all reactions formed heterogeneous mixtures throughout the reaction course. Therefore, it is not appropriate to compare the tendency of reactivity with method I conducted in THF, which effectively dissolves the generated $\mathbf{2_X}$. The lowest conversion of $\mathbf{1_{CN}}[BF_4]$ among the series of substrates may be explained in part by binding of the cyano group to the catalyst.[28,30,45]

Hydride elimination from substituted imidazolidines $\mathbf{2_X}$ was performed by utilizing 1 equiv of **8** and 1 mol % **4** at 25 °C (Table 6). Substrates with strongly electron-withdrawing

Table 6. Hydride Elimination from Asymmetrically Substituted Diphenylimidazolidines Catalyzed by 4[a]

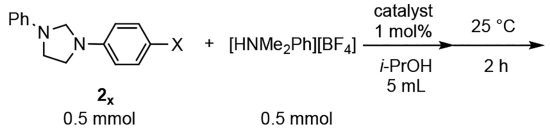

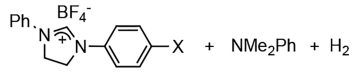

$\mathbf{1_X}[BF_4]$

entry	substrate	X	yield [%] $\mathbf{1_X}[BF_4]$[b]	H_2[c]
1	$\mathbf{2_F}$	F	92	85
2	$\mathbf{2_{Cl}}$	Cl	67	43
3	$\mathbf{2_{CF3}}$	CF_3	11	7
4	$\mathbf{2_{COOMe}}$	COOMe	0	1
5	$\mathbf{2_{CN}}$	CN	0	0
6	**2**	H	89	85
7	$\mathbf{2_{Me}}$	Me	63	58
8	$\mathbf{2_{OMe}}$	OMe	53	49

[a]Common reaction conditions: $\mathbf{2_X}$ (0.50 mmol), **8** (0.50 mmol), **4** (5 μmol), *i*PrOH (5 mL), 25 °C, 2 h, under vacuum. [b]Determined by ^1H NMR spectroscopy. [c]H_2 in the gas phase determined by GC analyses.

groups were poorly converted (entries 3−5), which was consistent with the prediction that these substituents electronically destabilize the cationic forms. While the reactivity of F-substituted $\mathbf{2_F}$ was similar to that of **2**, reactions of other substrates (entries 2, 7, 8) showed relatively poor conversion, regardless of the electronic nature of the substituents. Therefore, additional factors may determine reactivity such as solubility, proton acceptability, and tolerance of the catalyst to functional groups. Nevertheless, a number of imidazolinium derivatives were confirmed to allow reversible hydride addition and elimination associated with the uptake and release of H_2 by altering the proton concentration.

CONCLUSION

In this study, we used *N*,*N*′-diphenylimidazolinium cation $\mathbf{1}^+$ as a mimic of methenyltetrahydromethanopterin ($CH\text{-}H_4MPT^+$), the substrate for [Fe]-hydrogenase, and investigated its reversible reduction with H_2 into *N*,*N*′-diphenylimidazolidine **2** and a proton. Nonbiological noble metal complexes that activate H_2 heterolytically were examined in this model system. Hydride addition to $\mathbf{1}^+$ utilizing H_2 is practicable by conjugation with proton trapping, and accordingly, the conversion ratio is influenced by basic additives, whose basicity must not be less than lutidine to advance the reaction. We confirmed that NEt_3 is a suitable base, as it led to complete conversion into **2** with a

DOI: 10.1021/acs.inorgchem.7b00806
Inorg. Chem. XXXX, XXX, XXX−XXX

stoichiometric amount and caused no appreciable deprotonation of $\mathbf{1}^+$ to form the N-heterocyclic carbene. The examined catalysts exhibited satisfactory turnovers under ambient temperature and pressure. It is likely that all of these catalysts transfer the metal-bound hydride intermolecularly to the C-2 atom of the imidazolinium ring; this key step parallels one of the proposed mechanisms of [Fe]-hydrogenase reaction. Our bioinspired catalytic system supports that CH-H_4MPT$^+$ is a good acceptor of hydride, which can be generated from H_2 on transition metals under mild conditions. However, it should be kept in mind that the mechanisms of H_2 activation by these catalysts are not compatible with what occurs on the protein-bound FeGP cofactor.

The reverse conversion (**2** to $\mathbf{1}^+$) is promoted under opposite conditions: a stoichiometric amount of $HNMe_2Ph^+$ was added as a proton source in the representative experiments in this study. In contrast to the forward reaction ($\mathbf{1}^+$ to **2**), significant differences in activity and selectivity were observed between the catalysts. The most efficient catalyst was the Ir complex **4**, which produced $\mathbf{1}^+$ and H_2 with high selectivity and moderate turnover frequencies at room temperature. Its Ru analogue **3** exhibited the same selectivity but relatively slow reaction rates, similar to the forward reaction. Unexpectedly, the most active catalyst for the forward reaction in this study, **6**, promoted hydride elimination from **2** but evolved minimal H_2. A similar tendency was observed for **5**, and the existence of side reactions consuming the hydride was suspected. Additionally, reactions were accelerated in alcoholic media regardless of catalysts. This is in contrast with the catalyst-dependent solvent effects on the hydride transfer to $\mathbf{1}^+$, which is ascribed to the H_2 activation mechanism. The assistance of alcohol molecules in the hydride elimination step is postulated (Scheme 4), and these problems will be investigated in future studies. Finally, by using a complex catalyst **4**, a catalytic system utilizing H_2 to reversibly reduce $\mathbf{1}^+$ into **2** was successfully developed. This reaction model focusing on the substrates of [Fe]-hydrogenase (CH^+/CH_2-H_4MPT and H_2) may provide information regarding the roles of the H_4MPT cofactors.

EXPERIMENTAL SECTION

General Procedures. All the manipulations were performed using standard Schlenk techniques. Toluene, THF, and diethyl ether were purified by passing over columns of activated alumina and a supported copper catalyst supplied by Hansen & Co. Ltd., or they were dried using common procedures (CaH_2 for toluene and NaH for others) and distilled under nitrogen prior to use. Dichloromethane was dried and distilled over P_2O_5 and degassed under nitrogen before use. Dehydrated grade alcohols and acetonitrile were purchased from Wako Pure Chemical Industries. The catalyst precursor [(η^6-*p*-cymene)Ru((*R*,*R*)-Tsdpen−H)] (**3**; Tsdpen−H = (*p*-$MeC_6H_4SO_2$)-NCHPhCHPhNH) was commercially available from Kanto Chemical Co. and used as received. Other complexes [Cp*Ir((*R*,*R*)-Tsdpen−H)] (**4**; Cp* = η^5-C_5Me_5), [Cp*IrH((*R*,*R*)-Tsdpen)] (Tsdpen = (*p*-$MeC_6H_4SO_2$)NCHPhCHPhNH_2),[18b] [Cp*Ir(4-(1*H*-pyrazol-1-yl-κN^2)benzoic acid-κC^3)(H_2O)]$_2SO_4$ (**5**),[19] and [Tp^{Me2}Rh(1,2-S_2-C_6H_4)(MeCN)] (**6**; Tp^{Me2} = hydrotris(3,5-dimethylpyrazol-1-yl)-borate),[20] were synthesized as described previously. *N*,*N*′-Diphenylimidazolidine (**2**) was prepared by a previously described procedure[46] and recrystallized from hot ethanol. Unless otherwise indicated, all other reagents were obtained from commercial sources and were used without further purification. NMR spectra (^{1}H at 400 MHz and ^{13}C at 100.5 MHz) were recorded on a JEOL ECP-400 spectrometer at 20 °C, and chemical shifts were referenced using those of residual solvent resonances. IR spectra were obtained using a Thermo Scientific Nicolet iS10 FTIR Spectrometer equipped with a Thermo Scientific Smart iTR with a ZnSe crystal and were recorded over a wavenumber range of 600−3800 cm^{-1} with 2 cm^{-1} resolution. Elemental analyses were performed at The Microanalytical Laboratory, Department of Chemistry, Graduate School of Science, The University of Tokyo. GC analyses were carried out on a Shimadzu GC-14B gas chromatograph equipped with a TCD and stainless columns filled with molecular sieves 5A (mesh 60−80, 3.0 mm × 2.0 m) by using argon as the carrier gas.

Synthesis of Materials. The following compounds were prepared by reported procedures with some modifications.

*N,N′-Diphenylimidazolinium Tetrafluoroborate (**1**[BF_4]).*[47] *N*,*N*′-Diphenylethylenediamine (4.26 g, 20.1 mmol) and ammonium tetrafluoroborate (2.46 g, 23.1 mmol) were placed in a dried 50 mL Schlenk flask equipped with a magnetic stirring bar. The flask was evacuated and refilled with nitrogen gas three times. Under a stream of nitrogen, triethyl orthoformate (30 mL, 180 mmol) was added, and this mixture was refluxed for 5 h. After cooling to room temperature, the pale yellow precipitate was filtered off and repeatedly recrystallized three times from acetonitrile/EtOH to give colorless needles (2.85 g, 46% yield).

*2,6-Lutidinium Tetrafluoroborate (**7**).*[48] 2,6-Lutidine (2.00 mL, 17.2 mmol) was added dropwise to a mixture of HBF_4·Et_2O (2.00 mL, 14.5 mmol) and diethyl ether (20 mL) with vigorous stirring. A white precipitate was immediately formed, which was filtered and repeatedly washed with diethyl ether. Recrystallization of the remaining solid from dichloromethane (30 mL) and diethyl ether (100 mL) resulted in moderately hygroscopic colorless crystals (2.64 g, 93% yield).

*N,N-Dimethylanilinium Tetrafluoroborate (**8**).*[48,49] A dried Schlenk flask equipped with a magnetic stirring bar was evacuated and refilled with nitrogen gas three times. Under a stream of nitrogen, 25 mL of diethyl ether and *N*,*N*-dimethylaniline (2.8 mL, 22 mmol) were added to the flask. This solution was stirred with cooling at 0 °C, and HBF_4·Et_2O (3.0 mL, 22 mmol) was added dropwise. The colorless solid that had immediately deposited was crushed with a spatula, and the resulting mixture was gradually warmed to ambient temperature with stirring. After 1 h, the white precipitate was collected by filtration and repeatedly washed with diethyl ether. The solid was dissolved in dichloromethane (20 mL), and diethyl ether (60 mL) was layered on the filtered solution. After standing for 5 days, deposited colorless crystals were separated by filtration and dried *in vacuo* (2.64 g, 58% yield).

Hydride Addition Reaction. In a dry Schlenk flask (internal volume of 33−38 mL) equipped with a magnetic stirring bar, imidazolinium tetrafluoroborate ($\mathbf{1}_X$[BF_4], 0.500 mmol) was placed. The flask was repeatedly evacuated and refilled with nitrogen gas three times. Under a counterflow of nitrogen gas, solvent (5 mL) and organic base (0.50 mmol) were added through a syringe. The flask was sealed with a glass stopcock and degassed by two freeze−pump−thaw cycles using liquid nitrogen. As the mixture was kept frozen in a liquid nitrogen bath, the catalyst precursor was added to the flask under a counterflow of nitrogen. The flask was evacuated again at liquid nitrogen temperature and connected to a balloon filled with pure hydrogen gas. The reaction mixture was allowed to stir at a specific temperature and time. If the reaction was conducted in THF or dichloromethane, the gas phase was replaced with N_2 and triphenylmethane (ca. 0.5 mmol, accurately weighed) was added to the flask as an internal standard, followed by the addition of acetonitrile (2 mL) to form a homogeneous solution. If the solvent was alcohol or toluene, hydrogen gas and solvent were removed under high vacuum before adding triphenylmethane, and the mixture was dissolved completely by using dichloromethane and acetonitrile (total ca. 5 mL) under a nitrogen atmosphere. Approximately 0.5 mL of the solution was sampled, dried by rotary evaporation, and analyzed by ^{1}H NMR spectroscopy in acetonitrile-d_3.

Hydride Elimination Reaction. A dry Schlenk flask of a known internal volume (33−38 mL) was equipped with a magnetic stirring bar, and imidazolidine ($\mathbf{2}_X$, 0.500 mmol) and solvent (5 mL) were added under nitrogen. The flask was sealed with a glass stopcock, and freeze−pump−thaw degassing manipulation was carried out twice. While keeping the flask frozen at liquid nitrogen temperature, proton

DOI: 10.1021/acs.inorgchem.7b00806
Inorg. Chem. XXXX, XXX, XXX−XXX

reagent (0.500 mmol) and catalyst precursor were added under a counterflow of nitrogen gas. The flask was evacuated at −196 °C, and the reaction mixture was allowed to stir under the indicated conditions. After the reaction, the flask was backfilled with pure nitrogen gas to atmospheric pressure, and the gas phase was analyzed by gas chromatography (three measurements using 100 μL sample gas for each experiment). The partial pressure of H_2 in the apparatus was no more than 0.40 atm for each reaction. The amount of dissolved H_2 estimated using the Henry's constant was approximately 7 μmol at the maximum, which is much lower than that in the gas phase.[50] Thereafter, the organic materials were determined according to the procedure similar to that used in the above hydride addition reaction.

Sequential Hydride Addition and Elimination Reactions. A magnetic stirring bar and *N*,*N*′-diphenylimidazolinium tetrafluoroborate (**1**[BF_4]; 155 mg, 0.500 mmol) were placed in a Schlenk flask (33−38 mL internal volume accurately measured), and *i*PrOH (5 mL) and triethylamine (70 μL, 0.50 mmol) were added under a nitrogen atmosphere. After degassing the mixture by freeze−pump−thaw cycles, [Cp*Ir((*R*,*R*)-Tsdpen−H)] (**4**; 3.5 mg, 5.0 μmol, S/C = 100) was added to the frozen mixture under a nitrogen stream and the flask was evacuated at liquid nitrogen temperature. A balloon filled with pure hydrogen gas was connected to the flask, and the reaction mixture was stirred for 17 h at 25 °C. The resulting mixture was frozen in a liquid nitrogen bath, the gas phase was evacuated, and *N*,*N*-dimethylanilinium tetrafluoroborate (**8**; 104 mg, 0.50 mmol) was added under a counterflow of nitrogen. After evacuating the gas phase at −196 °C, the contents of the flask were allowed to stir at 25 °C for 2 h. Quantitative analysis of evolved H_2 and organic substances was carried out as described above.

Synthesis of *N*-Aryl-*N*′-phenyl-1,2-ethylenediamines. These compounds were prepared as described by Shafir et al.[51] (Method A: X = F, Cl, Me, OMe) or Wolfe et al.[52] (Method B: X = Br, CF_3, COOMe, CN) with some modifications.

Method A. To a Schlenk flask equipped with a magnetic stirring bar, *p*-substituted iodobenzene (10 mmol), CuI (95 mg, 0.5 mmol), and Cs_2CO_3 (6.5 g, 20 mmol) were added. When fluoroiodobenzene was reacted, it was added later with other liquid reagents. The flask was evacuated and refilled with nitrogen gas three times, and 2-isobutyrylcyclohexanone (0.3 mL, 2 mmol), *N*-phenylethylenediamine (1.6 mL, 12 mmol), and DMF (20 mL) were added through a syringe. The mixture was stirred at ambient temperature, and the reaction was monitored by using TLC until the iodobenzene derivative was consumed. The resulting mixture was filtered, and the filtrate was evaporated to dryness in a rotary evaporator. The products were purified by short column chromatography on silica gel eluted with dichloromethane. The obtained *N*-aryl-*N*′-phenylethylenediamine was used in the next step without further purification.

Method B. To a Schlenk flask equipped with a magnetic stirring bar, *p*-substituted bromobenzene (10 mmol) and *N*-phenylethylenediamine (1.6 mL, 12 mmol) were added. After the flask was evacuated and refilled with nitrogen gas three times, toluene (20 mL) was added. To this solution, Pd(dibenzalacetone)$_2$ (0.1 mmol), 2,2′-bis(diphenylphosphino)-1,1′-binaphthyl (0.1 mmol), and *t*-BuONa (14 mmol) were added, and the mixture was heated at 100 °C. After full conversion of the bromobenzene derivative (checked by TLC), the reaction mixture was filtered, and the filtrate was evaporated to dryness in a rotary evaporator. The products were purified by short column chromatography on silica gel eluted with dichloromethane. The obtained *N*-aryl-*N*′-phenylethylenediamine was used in the next step without further purification.

Synthesis of *N*-Aryl-*N*′-phenylimidazolinium tetrafluoroborates. Crude *N*-aryl-*N*′-phenyl-1,2-ethylenediamine prepared as described above (up to 10 mmol) was mixed with triethylorthoformate (15 mL, 90 mmol) and ammonium tetrafluoroborate (1.15 g, 11 mmol), and the mixture was refluxed for 5 h. After cooling to room temperature, the yellowish white precipitate was filtered off and recrystallized from MeCN/EtOH or DMF/EtOH. Characterization data for these new compounds are included in the Supporting Information.

Synthesis of *N*-Aryl-*N*′-phenylimidazolidines. These compounds were synthesized as described in the literature[53] with some modifications. Crude *N*-aryl-*N*′-phenyl-1,2-ethylenediamine prepared as described above (up to 10 mmol) was dissolved in 50 mL of methanol. Excess 37% aqueous formaldehyde (10 mL, 130 mmol) and formic acid (0.5 mL, 13 mmol) were added to this solution. The colorless solid precipitated immediately, and the resulting mixture was stirred for 3 h at room temperature. The precipitate was filtered off and recrystallized from hot ethanol, followed by vacuum drying. Characterization data for these new compounds are included in the Supporting Information.

■ ASSOCIATED CONTENT

Supporting Information

The Supporting Information is available free of charge on the ACS Publications website at DOI: 10.1021/acs.inorgchem.7b00806.

Additional experimental data for hydride addition to **1**[BF_4] under H_2 utilizing various catalysts and deuterated solvents, and spectroscopic and microanalytical data of imidazolinium salts and imidazolidines (PDF)

■ AUTHOR INFORMATION

Corresponding Author

*E-mail: seino@gipc.akita-u.ac.jp. Fax: +81-18-889-2589.

ORCID

Masahiro Hatazawa: 0000-0002-4260-2830

Hidetake Seino: 0000-0002-8792-1974

Notes

The authors declare no competing financial interest.

■ ACKNOWLEDGMENTS

This work was supported by JSPS KAKENHI Grant Numbers 21350033 (B) and 25410108 (C). M.H. acknowledges financial support from JSPS through the Program for Leading Graduate Schools (MERIT).

■ REFERENCES

(1) (a) Shima, S.; Warkentin, E.; Thauer, R. K.; Ermler, U. Structure and function of enzymes involved in the methanogenic pathway utilizing carbon dioxide and molecular hydrogen. *J. Biosci. Bioeng.* **2002**, *93*, 519−530. (b) Thauer, R. K.; Kaster, A.-K.; Seedorf, H.; Buckel, W.; Hedderich, R. Methanogenic archaea: ecologically relevant differences in energy conservation. *Nat. Rev. Microbiol.* **2008**, *6*, 579−591. (c) Lessner, D. J. *Encyclopedia of Life Sciences*; John Wiley & Sons: Chichester, U.K., 2009.

(2) Reviews: (a) Shima, S.; Ermler, U. Structure and Function of [Fe]-Hydrogenase and its Iron−Guanylylpyridinol (FeGP) Cofactor. *Eur. J. Inorg. Chem.* **2011**, *2011*, 963−972. (b) Shima, S.; Thauer, R. K. A third type of hydrogenase catalyzing H_2 activation. *Chem. Rec.* **2007**, *7*, 37−46. (c) Dey, S.; Das, P. K.; Dey, A. Mononuclear iron hydrogenase. *Coord. Chem. Rev.* **2013**, *257*, 42−43. (d) Corr, M. J.; Murphy, J. A. Evolution in the understanding of [Fe]-hydrogenase. *Chem. Soc. Rev.* **2011**, *40*, 2279−2292.

(3) Recent works: (a) Shima, S.; Vogt, S.; Göbels, A.; Bill, E. Iron-Chromophore Circular Dichroism of [Fe]-Hydrogenase: The Conformational Change Required for H_2 Activation. *Angew. Chem., Int. Ed.* **2010**, *49*, 9917−9921. (b) Schick, M.; Xie, X.; Ataka, K.; Kahnt, J.; Linne, U.; Shima, S. Biosynthesis of the Iron-Guanylylpyridinol Cofactor of [Fe]-Hydrogenase in Methanogenic Archaea as Elucidated by Stable-Isotope Labeling. *J. Am. Chem. Soc.* **2012**, *134*, 3271−3280. (c) Shima, S.; Chen, D.; Xu, T.; Wodrich, M. D.; Fujishiro, T.; Schultz, K. M.; Kahnt, J.; Ataka, K.; Hu, X.

DOI: 10.1021/acs.inorgchem.7b00806
Inorg. Chem. XXXX, XXX, XXX−XXX

Reconstitution of [Fe]-hydrogenase using model complexes. *Nat. Chem.* **2015**, *7*, 995−1002.
(4) (a) Shima, S.; Pilak, O.; Vogt, S.; Schick, M.; Stagni, M. S.; Meyer-Klaucke, W.; Warkentin, E.; Thauer, R. K.; Ermler, U. The Crystal Structure of [Fe]-Hydrogenase Reveals the Geometry of the Active Site. *Science* **2008**, *321*, 572−575. (b) Hiromoto, T.; Ataka, K.; Pilak, O.; Vogt, S.; Stagni, M. S.; Meyer-Klaucke, W.; Warkentin, E.; Thauer, R. K.; Shima, S.; Ermler, U. The crystal structure of C176A mutated [Fe]-hydrogenase suggests an acyl-iron ligation in the active site iron complex. *FEBS Lett.* **2009**, *583*, 585−590. (c) Hiromoto, T.; Warkentin, E.; Moll, J.; Ermler, U.; Shima, S. The Crystal Structure of an [Fe]-Hydrogenase−Substrate Complex Reveals the Framework for H_2 Activation. *Angew. Chem., Int. Ed.* **2009**, *48*, 6457−6460. (d) Shima, S.; Schick, M.; Kahnt, J.; Ataka, K.; Steinbach, K.; Linne, U. Evidence for acyl−iron ligation in the active site of [Fe]-hydrogenase provided by mass spectrometry and infrared spectroscopy. *Dalton Trans.* **2012**, *41*, 767−771. (e) Tamura, H.; Salomone-Stagni, M.; Fujishiro, T.; Warkentin, E.; Meyer-Klaucke, W.; Ermler, U.; Shima, S. Crystal Structures of [Fe]-Hydrogenase in Complex with Inhibitory Isocyanides: Implications for the H_2-Activation Site. *Angew. Chem., Int. Ed.* **2013**, *52*, 9656−9659.
(5) (a) Vignais, P. M.; Billoud, B. Occurrence, Classification, and Biological Function of Hydrogenases: An Overview. *Chem. Rev.* **2007**, *107*, 4206−4272. (b) De Lacey, A. L.; Fernández, V. M.; Rousset, M.; Cammack, R. Activation and Inactivation of Hydrogenase Function and the Catalytic Cycle: Spectroelectrochemical Studies. *Chem. Rev.* **2007**, *107*, 4304−4330. (c) Thauer, R. K.; Kaster, A.-K.; Goenrich, M.; Schick, M.; Hiromoto, T.; Shima, S. Hydrogenases from Methanogenic Archaea, Nickel, a Novel Cofactor, and H_2 Storage. *Annu. Rev. Biochem.* **2010**, *79*, 507−36. (d) Lubitz, W.; Ogata, H.; Rüdiger, O.; Reijerse, E. Hydrogenases. *Chem. Rev.* **2014**, *114*, 4081−4148.
(6) Yang, X.; Hall, M. B. Monoiron Hydrogenase Catalysis: Hydrogen Activation with the Formation of a Dihydrogen, Fe−$H^{\delta-}\cdots H^{\delta+}$−O, Bond and Methenyl-$H_4MPT^+$ Triggered Hydride Transfer. *J. Am. Chem. Soc.* **2009**, *131*, 10901−10908.
(7) (a) Finkelmann, A. R.; Stiebritz, M. T.; Reiher, M. Kinetic Modeling of Hydrogen Conversion at [Fe] Hydrogenase Active-Site Models. *J. Phys. Chem. B* **2013**, *117*, 4806−4817. (b) Finkelmann, A. R.; Senn, H. M.; Reiher, M. Hydrogen-activation mechanism of [Fe] hydrogenase revealed by multi-scale modeling. *Chem. Sci.* **2014**, *5*, 4474−4482.
(8) A computational study on the [Fe]-hydrogenase biomimetics: Murray, K. A.; Wodrich, M. D.; Hu, X.; Corminboeuf, C. Toward Functional Type III [Fe]-Hydrogenase Biomimics for H_2 Activation: Insights from Computation. *Chem. - Eur. J.* **2015**, *21*, 3987−3996.
(9) Reviews: (a) Wright, J. A.; Turrell, P. J.; Pickett, C. J. The Third Hydrogenase: More Natural Organometallics. *Organometallics* **2010**, *29*, 6146−6156. (b) Schultz, K. M.; Chen, D.; Hu, X. [Fe]-Hydrogenase and Models that Contain Iron−Acyl Ligation. *Chem. - Asian J.* **2013**, *8*, 1068−1075. (c) Schilter, D.; Camara, J. M.; Huynh, M. T.; Hammes-Schiffer, S.; Rauchfuss, T. B. Hydrogenase Enzymes and Their Synthetic Models: The Role of Metal Hydrides. *Chem. Rev.* **2016**, *116*, 8693−8749.
(10) (a) Turrell, P. J.; Wright, J. A.; Peck, J. N. T.; Oganesyan, V. S.; Pickett, C. J. The Third Hydrogenase: A Ferracyclic Carbamoyl with Close Structural Analogy to the Active Site of Hmd. *Angew. Chem., Int. Ed.* **2010**, *49*, 7508−7511. (b) Royer, A. M.; Salomone-Stagni, M.; Rauchfuss, T. B.; Meyer-Klaucke, W. Iron Acyl Thiolato Carbonyls: Structural Models for the Active Site of the [Fe]-Hydrogenase (Hmd). *J. Am. Chem. Soc.* **2010**, *132*, 16997−17003. (c) Tanino, S.; Ohki, Y.; Tatsumi, K. An Iron(II) Carbonyl Thiolato Complex Bearing 2-Methoxy-Pyridine: A Structural Model of the Active Site of [Fe] Hydrogenase. *Chem. - Asian J.* **2010**, *5*, 1962−1964. (d) Liu, T.; Li, B.; Popescu, C. V.; Bilko, A.; Pérez, L. M.; Hall, M. B.; Darensbourg, M. Y. Analysis of a Pentacoordinate Iron Dicarbonyl as Synthetic Analogue of the Hmd or Mono-Iron Hydrogenase Active Site. *Chem. - Eur. J.* **2010**, *16*, 3083−3089. (e) Song, L.-C.; Hu, F.-Q.; Zhao, G.-Y.; Zhang, J.-W.; Zhang, W.-W. Several New [Fe]Hydrogenase Model Complexes with a Single Fe Center Ligated to an Acylmethyl(hydroxymethyl)-pyridine or Acylmethyl(hydroxy)pyridine Ligand. *Organometallics* **2014**, *33*, 6614−6622. (f) Durgaprasad, G.; Xie, Z.-L.; Rose, M. J. Iron Hydride Detection and Intramolecular Hydride Transfer in a Synthetic Model of Mono-Iron Hydrogenase with a CNS Chelate. *Inorg. Chem.* **2016**, *55*, 386−389. (g) Song, L.-C.; Xu, K.-K.; Han, X.-F.; Zhang, J.-W. Synthetic and Structural Studies of 2-Acylmethyl-6-R-Difunctionalized Pyridine Ligand-Containing Iron Complexes Related to [Fe]-Hydrogenase. *Inorg. Chem.* **2016**, *55*, 1258−1269. (h) Xu, T.; Yin, C.-J. M.; Wodrich, M. D.; Mazza, S.; Schultz, K. M.; Scopelliti, R.; Hu, X. A Functional Model of [Fe]-Hydrogenase. *J. Am. Chem. Soc.* **2016**, *138*, 3270−3273. (i) Seo, J.; Manes, T. A.; Rose, M. J. Structural and functional synthetic model of monoiron hydrogenase featuring an anthracene scaffold. *Nat. Chem.* **2017**, *9*, 552−557.
(11) Royer, A. M.; Rauchfuss, T. B.; Wilson, S. R. Coordination Chemistry of a Model for the GP Cofactor in the Hmd Hydrogenase: Hydrogen-Bonding and Hydrogen-Transfer Catalysis. *Inorg. Chem.* **2008**, *47*, 395−397.
(12) Corr, M. J.; Gibson, K. F.; Kennedy, A. R.; Murphy, J. A. Amidine Dications: Isolation and [Fe]-Hydrogenase-Related Hydrogenation. *J. Am. Chem. Soc.* **2009**, *131*, 9174−9175.
(13) Kalz, K. F.; Brinkmeier, A.; Dechert, S.; Mata, R. A.; Meyer, F. Functional Model for the [Fe] Hydrogenase Inspired by the Frustrated Lewis Pair Concept. *J. Am. Chem. Soc.* **2014**, *136*, 16626−16634.
(14) (a) Kubas, G. J. Fundamentals of H_2 Binding and Reactivity on Transition Metals Underlying Hydrogenase Function and H_2 Production and Storage. *Chem. Rev.* **2007**, *107*, 4152−4205. (b) Tard, C.; Pickett, C. J. Structural and Functional Analogues of the Active Sites of the [Fe]-, [NiFe]-, and [FeFe]-Hydrogenases. *Chem. Rev.* **2009**, *109*, 2245−2274. (c) Xu, T.; Chen, D.; Hu, X. Hydrogen-activating models of hydrogenases. *Coord. Chem. Rev.* **2015**, *303*, 32−41.
(15) Teles, J. H.; Brode, S.; Berkessel, A. Hydrogenation without a Metal Catalyst: An ab Initio Study on the Mechanism of the Metal-Free Hydrogenase from *Methanobacterium thermoautotrophicum*. *J. Am. Chem. Soc.* **1998**, *120*, 1345−1346.
(16) (a) Noyori, R.; Hashiguchi, S. Asymmetric Transfer Hydrogenation Catalyzed by Chiral Ruthenium Complexes. *Acc. Chem. Res.* **1997**, *30*, 97−102. (b) Ikariya, T.; Murata, K.; Noyori, R. Bifunctional transition metal-based molecular catalysts for asymmetric syntheses. *Org. Biomol. Chem.* **2006**, *4*, 393−406. (c) Grützmacher, H. Cooperating Ligands in Catalysis. *Angew. Chem., Int. Ed.* **2008**, *47*, 1814−1818. (d) Gunanathan, C.; Milstein, D. Metal−Ligand Cooperation by Aromatization−Dearomatization: A New Paradigm in Bond Activation and "Green" Catalysis. *Acc. Chem. Res.* **2011**, *44*, 588−602. (e) Dub, P. A.; Ikariya, T. Catalytic Reductive Transformations of Carboxylic and Carbonic Acid Derivatives Using Molecular Hydrogen. *ACS Catal.* **2012**, *2*, 1718−1841. (f) Askevold, B.; Roesky, H. W.; Schneider, S. Learning from the Neighbors: Improving Homogeneous Catalysts with Functional Ligands Motivated by Heterogeneous and Biocatalysis. *ChemCatChem* **2012**, *4*, 307−320. (g) Morris, R. H. Exploiting Metal−Ligand Bifunctional Reactions in the Design of Iron Asymmetric Hydrogenation Catalysts. *Acc. Chem. Res.* **2015**, *48*, 1494−1502.
(17) (a) Hashiguchi, S.; Fujii, A.; Takehara, J.; Ikariya, T.; Noyori, R. Asymmetric Transfer Hydrogenation of Aromatic Ketones Catalyzed by Chiral Ruthenium(II) Complexes. *J. Am. Chem. Soc.* **1995**, *117*, 7562−7563. (b) Haack, K.-J.; Hashiguchi, S.; Fujii, A.; Ikariya, T.; Noyori, R. The Catalyst Precursor, Catalyst, and Intermediate in the Ru^{II}-Promoted Asymmetric Hydrogen Transfer between Alcohols and Ketones. *Angew. Chem., Int. Ed. Engl.* **1997**, *36*, 285−288.
(18) (a) Mashima, K.; Abe, T.; Tani, K. Asymmetric Transfer Hydrogenation of Ketonic Substrates Catalyzed by (η^5-C_5Me_5)MCl Complexes (M = Rh and Ir) of (1*S*,2*S*)-*N*-(*p*-Toluenesulfonyl)-1,2-diphenylethylenediamine. *Chem. Lett.* **1998**, *27*, 1199−1201. (b) Mashima, K.; Abe, T.; Tani, K. The Half-sandwich Hydride and 16-Electron Complexes of Rhodium and Iridium Containing (1*S*,2*S*)-*N*-(*p*-Toluenesulfonyl)-1,2-diphenylethylenediamine: Relevant to the Asymmetric Transfer Hydrogenation. *Chem. Lett.* **1998**, *27*, 1201−1202. (c) Murata, K.; Ikariya, T.; Noyori, R. New Chiral Rhodium and

DOI: 10.1021/acs.inorgchem.7b00806
Inorg. Chem. XXXX, XXX, XXX−XXX

Iridium Complexes with Chiral Diamine Ligands for Asymmetric Transfer Hydrogenation of Aromatic Ketones. *J. Org. Chem.* **1999**, *64*, 2186−2187.
(19) Maenaka, Y.; Suenobu, T.; Fukuzumi, S. Efficient Catalytic Interconversion between NADH and NAD^+ Accompanied by Generation and Consumption of Hydrogen with a Water-Soluble Iridium Complex at Ambient Pressure and Temperature. *J. Am. Chem. Soc.* **2012**, *134*, 367−374.
(20) (a) Misumi, Y.; Seino, H.; Mizobe, Y. Heterolytic Cleavage of Hydrogen Molecule by Rhodium Thiolate Complexes That Catalyze Chemoselective Hydrogenation of Imines under Ambient Conditions. *J. Am. Chem. Soc.* **2009**, *131*, 14636−14637. (b) Seino, H.; Misumi, Y.; Hojo, Y.; Mizobe, Y. Heterolytic H_2 activation by rhodium thiolato complexes bearing the hydrotris(pyrazolyl)borato ligand and application to catalytic hydrogenation under mild conditions. *Dalton Trans.* **2010**, *39*, 3072−3082.
(21) Jaenicke, L.; Brode, E. Modelluntersuchungen zur biologischen Aktivierung der Einkohlenstoff-Einheiten, I *N.N′*-Diaryl-äthylendiamine als Modelle der Tetrahydrofolsäure in nicht-enzymatischen Reaktionen. *Justus Liebigs Ann. Chem.* **1959**, *624*, 120−136.
(22) Salerno, A.; Ceriani, V.; Perillo, I. A. Reduction of substituted 1*H*-4,5-dihydroimidazolium salts. *J. Heterocycl. Chem.* **1992**, *29*, 1725−1733.
(23) Arduengo, A. J., III; Krafczyk, R.; Schmutzler, R.; Craig, H. A.; Goerlich, J. R.; Marshall, W. J.; Unverzagt, M. Imidazolylidenes, imidazolinylidenes and imidazolidines. *Tetrahedron* **1999**, *55*, 14523−14534.
(24) (a) Catalytic hydrogenation of imidazolin-2-ylidenes (saturated NHCs) to imidazolidines under 1 atm H_2 by using Pd or Pt metal has been reported.[24b] Stoichiometric conversion of a saturated NHC dimer into the corresponding imidazolidine has been achieved under forcing conditions without catalysts by using benzenethiol as a reducing agent.[24c] (b) Denk, M. K.; Rodezno, J. M.; Gupta, S.; Lough, A. J. Synthesis and reactivity of subvalent compounds: Part 11. Oxidation, hydrogenation and hydrolysis of stable diamino carbenes. *J. Organomet. Chem.* **2001**, *617*−*618*, 242−253. (c) Schönberg, A.; Singer, E.; Stephan, W. C═C-Doppelbindungen mit extremer Reaktivität, IV. Ungewöhnliche Reaktionen mit Thiophenol, 1,2-Ethandithiol und anderen schwefelhaltigen Verbindungen. *Chem. Ber.* **1984**, *117*, 3388−3399.
(25) Garrido, G.; Koort, E.; Ràfols, C.; Bosch, E.; Rodima, T.; Leito, I.; Rosés, M. Acid−Base Equilibria in Nonpolar Media. Absolute pK_a Scale of Bases in Tetrahydrofuran. *J. Org. Chem.* **2006**, *71*, 9062−9067.
(26) (a) Samec, J. S. M.; Bäckvall, J.-E.; Andersson, P. G.; Brandt, P. Mechanistic aspects of transition metal-catalyzed hydrogen transfer reactions. *Chem. Soc. Rev.* **2006**, *35*, 237−248. (b) Ikariya, T.; Blacker, A. J. Asymmetric Transfer Hydrogenation of Ketones with Bifunctional Transition Metal-Based Molecular Catalysts. *Acc. Chem. Res.* **2007**, *40*, 1300−1308.
(27) Åberg, J. B.; Samec, J. S. M.; Bäckvall, J.-E. Mechanistic investigation on the hydrogenation of imines by [*p*-(Me_2CH)-C_6H_4Me]RuH($NH_2CHPhCHPhNSO_2C_6H_4$-*p*-CH_3). Experimental support for an ionic pathway. *Chem. Commun.* **2006**, 2771−2773.
(28) Shirai, S.; Nara, H.; Kayaki, Y.; Ikariya, T. Remarkable Positive Effect of Silver Salts on Asymmetric Hydrogenation of Acyclic Imines with Cp*Ir Complexes Bearing Chiral N-Sulfonylated Diamine Ligands. *Organometallics* **2009**, *28*, 802−809.
(29) Reaction of **A** with Ph_3C^+ exclusively produces Ph_3CH.[30]
(30) Heiden, Z. M.; Rauchfuss, T. B. Proton-Induced Lewis Acidity of Unsaturated Iridium Amides. *J. Am. Chem. Soc.* **2006**, *128*, 13048−13049.
(31) Heiden, Z. M.; Rauchfuss, T. B. Proton-Assisted Activation of Dihydrogen: Mechanistic Aspects of Proton-Catalyzed Addition of H_2 to Ru and Ir Amido Complexes. *J. Am. Chem. Soc.* **2009**, *131*, 3593−3600.
(32) (a) Ito, M.; Hirakawa, M.; Murata, K.; Ikariya, T. Hydrogenation of Aromatic Ketones Catalyzed by (η^5-$C_5(CH_3)_5$)Ru Complexes Bearing Primary Amines. *Organometallics* **2001**, *20*, 379−381. (b) Casey, C. P.; Johnson, J. B.; Singer, S. W.; Cui, Q. Hydrogen Elimination from a Hydroxycyclopentadienyl Ruthenium(II) Hydride: Study of Hydrogen Activation in a Ligand−Metal Bifunctional Hydrogenation Catalyst. *J. Am. Chem. Soc.* **2005**, *127*, 3100−3109. (c) Hedberg, C.; Källström, K.; Arvidsson, P. I.; Brandt, P.; Andersson, P. G. Mechanistic Insights into the Phosphine-Free RuCp*-Diamine-Catalyzed Hydrogenation of Aryl Ketones: Experimental and Theoretical Evidence for an Alcohol-Mediated Dihydrogen Activation. *J. Am. Chem. Soc.* **2005**, *127*, 15083−15090. (d) Moritani, J.; Kayaki, Y.; Ikariya, T. Advantageous asymmetric ketone reduction with a competitive hydrogenation/transfer hydrogenation system using chiral bifunctional iridium catalysts. *RSC Adv.* **2014**, *4*, 61001−61004. (e) Matsunami, A.; Kayaki, Y.; Ikariya, T. Enhanced Hydrogen Generation from Formic Acid by Half-Sandwich Iridium(III) Complexes with Metal/NH Bifunctionality: A Pronounced Switch from Transfer Hydrogenation. *Chem. - Eur. J.* **2015**, *21*, 13513−13517.
(33) Poyatos, M.; Prades, A.; Gonell, S.; Gusev, D. G.; Peris, E. Imidazolidines as hydride sources for the formation of late transition-metal monohydrides. *Chem. Sci.* **2012**, *3*, 1300−1303.
(34) Csihony, S.; Culkin, D. A.; Sentman, A. C.; Dove, A. P.; Waymouth, R. M.; Hedrick, J. L. Single-Component Catalyst/Initiators for the Organocatalytic Ring-Opening Polymerization of Lactide. *J. Am. Chem. Soc.* **2005**, *127*, 9079−9084.
(35) McSkimming, A.; Colbran, S. B. The coordination chemistry of organo-hydride donors: new prospects for efficient multi-electron reduction. *Chem. Soc. Rev.* **2013**, *42*, 5439−5488.
(36) (a) Reactions of imidazolidines as hydride donor or reductant have been long known except for those evolving H_2.[21,36b−d] (b) Rabe, E.; Wanzlick, H.-W. Dehydrierung von 1,3-Diaryl-imidazolidinen mit Tetrachlorkohlenstoff. *Liebigs Ann. Chem.* **1973**, *1973*, 40−44. (c) Rabe, E.; Wanzlick, H.-W. Dehydrierung von 1,3-Diphenylimidazolidinen mit Chinonen und Azoverbindungen. *Liebigs Ann. Chem.* **1975**, *1975*, 195−200. (d) Brunet, P.; Wuest, J. D. Formal transfers of hydride from carbon−hydrogen bonds. Attempted generation of H_2 by intramolecular protonolyses of the activated carbon−hydrogen bonds of dihydrobenzimidazoles. *Can. J. Chem.* **1996**, *74*, 689−696.
(37) Schwarz, D. E.; Cameron, T. M.; Hay, P. J.; Scott, B. L.; Tumas, W.; Thorn, D. L. Hydrogen evolution from organic "hydrides". *Chem. Commun.* **2005**, 5919−5921.
(38) (a) This reaction has been performed in MeCN, in which the pK_a value of acetic acid is 23.5.[38b] It has been claimed that pK_a's of neutral Brønsted acids drastically increase in MeCN as compared with aqueous media.[38c] (b) Kütt, A.; Leito, I.; Kaljurand, I.; Sooväli, L.; Vlasov, V. M.; Yagupolskii, L. M.; Koppel, I. A. A Comprehensive Self-Consistent Spectrophotometric Acidity Scale of Neutral Brønsted Acids in Acetonitrile. *J. Org. Chem.* **2006**, *71*, 2829−2838. (c) Sarmini, K.; Kenndler, E. Ionization constants of weak acids and bases in organic solvents. *J. Biochem. Biophys. Methods* **1999**, *38*, 123−137.
(39) (a) Zhu, X.-Q.; Zhang, M.-T.; Yu, A.; Wang, C.-H.; Cheng, J.-P. Hydride, Hydrogen Atom, Proton, and Electron Transfer Driving Forces of Various Five-Membered Heterocyclic Organic Hydrides and Their Reaction Intermediates in Acetonitrile. *J. Am. Chem. Soc.* **2008**, *130*, 2501−2516. (b) Richter, D.; Tan, Y.; Antipova, A.; Zhu, X.-Q.; Mayr, H. Kinetics of Hydride Abstractions from 2-Arylbenzimidazolines. *Chem. - Asian J.* **2009**, *4*, 1824−1829. (c) Zhu, X.-Q.; Deng, F.-H.; Yang, J.-D.; Li, X.-T.; Chen, Q.; Lei, N.-P.; Meng, F.-K.; Zhao, X.-P.; Han, S.-H.; Hao, E.-J.; Mu, Y. Y. A classical but new kinetic equation for hydride transfer reactions. *Org. Biomol. Chem.* **2013**, *11*, 6071−6089.
(40) Hydrogen evolution from *N,N′*-dimethylbenzimidazoline and acetic acid catalyzed by [$RhCl(PPh_3)_3$] barely occurs under forcing conditions (TOF = 117 h^{-1} at 70 °C).[37]
(41) (a) Eberle, U.; Felderhoff, M.; Schüth, F. Chemical and Physical Solutions for Hydrogen Storage. *Angew. Chem., Int. Ed.* **2009**, *48*, 6608−6630. (b) Makowski, P.; Thomas, A.; Kuhn, P.; Goettmann, F. Organic materials for hydrogen storage applications: from physisorption on organic solids to chemisorption in organic molecules. *Energy Environ. Sci.* **2009**, *2*, 480−490. (c) Trincado, M.; Banerjee, D.; Grützmacher, H. Molecular catalysts for hydrogen production from alcohols. *Energy Environ. Sci.* **2014**, *7*, 2464−2503. (d) Zhu, Q.-L.; Xu,

DOI: 10.1021/acs.inorgchem.7b00806
Inorg. Chem. XXXX, XXX, XXX−XXX

Q. Liquid organic and inorganic chemical hydrides for high-capacity hydrogen storage. *Energy Environ. Sci.* **2015**, *8*, 478−512.
(42) (a) Wang, Z.; Tonks, I.; Belli, J.; Jensen, C. M. Dehydrogenation of *N*-ethyl perhydrocarbazole catalyzed by PCP pincer iridium complexes: Evaluation of a homogenous hydrogen storage system. *J. Organomet. Chem.* **2009**, *694*, 2854−2857. (b) Hull, J. F.; Himeda, Y.; Wang, W.-H.; Hashiguchi, B.; Periana, R.; Szalda, D. J.; Muckerman, J. T.; Fujita, E. Reversible hydrogen storage using CO_2 and a proton-switchable iridium catalyst in aqueous media under mild temperatures and pressures. *Nat. Chem.* **2012**, *4*, 383−388. (c) Kawahara, R.; Fujita, K.; Yamaguchi, R. Cooperative Catalysis by Iridium Complexes with a Bipyridonate Ligand: Versatile Dehydrogenative Oxidation of Alcohols and Reversible Dehydrogenation−Hydrogenation between 2-Propanol and Acetone. *Angew. Chem., Int. Ed.* **2012**, *51*, 12790−12794. (d) Fujita, K.; Tanaka, Y.; Kobayashi, M.; Yamaguchi, R. Homogeneous Perdehydrogenation and Perhydrogenation of Fused Bicyclic N-Heterocycles Catalyzed by Iridium Complexes Bearing a Functional Bipyridonate Ligand. *J. Am. Chem. Soc.* **2014**, *136*, 4829−4832. (e) Hu, P.; Fogler, E.; Diskin-Posner, Y.; Iron, M. A.; Milstein, D. A novel liquid organic hydrogen carrier system based on catalytic peptide formation and hydrogenation. *Nat. Commun.* **2015**, *6*, 6859.
(43) (a) Maden, B. E. H. Tetrahydrofolate and tetrahydromethanopterin compared: functionally distinct carriers in C_1 metabolism. *Biochem. J.* **2000**, *350*, 609−629. (b) Acharya, P.; Goenrich, M.; Hagemeier, C. H.; Demmer, U.; Vorholt, J. A.; Thauer, R. K.; Ermler, U. How an Enzyme Binds the C_1 Carrier Tetrahydromethanopterin: Structure of the Tetrahydromethanopterin-Dependent Formaldehyde-Activating Enzyme (Fae) from *Methylobacterium extorquens* AM1. *J. Biol. Chem.* **2005**, *280*, 13712−13719.
(44) The numbering scheme generally adopted for H_4folate is used here: Poe, M.; Benkovic, S. J. 5-Formyl- and 10-formyl-5,6,7,8-tetrahydrofolate. Conformation of the tetrahydropyrazine ring and formyl group in solution. *Biochemistry* **1980**, *19*, 4576−4582.
(45) Heiden, Z. M.; Gorecki, B. J.; Rauchfuss, T. B. Lewis Base Adducts Derived from Transfer Hydrogenation Catalysts: Scope and Selectivity. *Organometallics* **2008**, *27*, 1542−1549.
(46) Denk, M. K.; Gupta, S.; Brownie, J.; Tajammul, S.; Lough, A. J. C−H Activation with Elemental Sulfur: Synthesis of Cyclic Thioureas from Formaldehyde Aminals and S_8. *Chem. - Eur. J.* **2001**, *7*, 4477−4486.
(47) Saba, S.; Brescia, A.; Kaloustian, M. K. One-pot synthesis of cyclic amidinium tetrafluoroborates and hexafluorophosphates; the simplest models of N^5,N^{10}-methenyltetrahydrofolate coenzyme. *Tetrahedron Lett.* **1991**, *32*, 5031−5034.
(48) Santoro, F.; Althaus, M.; Bonaccorsi, C.; Gischig, S.; Mezzetti, A. Acidic Ruthenium PNNP Complexes of Non-enolized 1,3-Dicarbonyl Compounds as Catalysts for Asymmetric Michael Addition. *Organometallics* **2008**, *27*, 3866−3878.
(49) McCarthy, B. D.; Martin, D. J.; Rountree, E. S.; Ullman, A. C.; Dempsey, J. L. Electrochemical Reduction of Brønsted Acids by Glassy Carbon in Acetonitrile—Implications for Electrocatalytic Hydrogen Evolution. *Inorg. Chem.* **2014**, *53*, 8350−8361.
(50) (a) Henry's constants of H_2 at 25 °C are 3.33 (THF),[50b] 3.50 (EtOH),[50c] 3.46 (*i*PrOH),[50d] and 2.96 (toluene)[50b] mmol/L·atm. Some of these values are converted from related constants in the original reports. (b) Brunner, E. Solubility of hydrogen in 10 organic solvents at 298.15, 323.15, and 373.15 K. *J. Chem. Eng. Data* **1985**, *30*, 269−273. (c) Katayama, T.; Nitta, T. Solubilities of hydrogen and nitrogen in alcohols and *n*-hexane. *J. Chem. Eng. Data* **1976**, *21*, 194−196. (d) Puri, P. S.; Ruether, J. A. Additive excess free energy models for predicting gas solubilities in mixed solvents. *Can. J. Chem. Eng.* **1974**, *52*, 636−640.
(51) Shafir, A.; Buchwald, S. L. Highly Selective Room-Temperature Copper-Catalyzed C−N Coupling Reactions. *J. Am. Chem. Soc.* **2006**, *128*, 8742−8743.
(52) Wolfe, J. P.; Wagaw, S.; Buchwald, S. L. An Improved Catalyst System for Aromatic Carbon−Nitrogen Bond Formation: The Possible Involvement of Bis(Phosphine) Palladium Complexes as Key Intermediates. *J. Am. Chem. Soc.* **1996**, *118*, 7215−7216.
(53) Lambert, J. B.; Huseland, D. E.; Wang, G. Synthesis of 1,3-Disubstituted Diazolidines. *Synthesis* **1986**, *1986*, 657−658.

DOI: 10.1021/acs.inorgchem.7b00806
Inorg. Chem. XXXX, XXX, XXX−XXX